X-ray Diffraction

applied to the study of polycrystalline materials

Prof. Paolo Scardi

Department of Materials Engineering and Industrial Technologies, University of Trento

These slides were used during the ICTP School on Synchrotron Radiation and Applications – Gargnano (TS), May 15th 2006. They are part of the X-ray Diffraction course for the PhD programme in Materials Engineering at the University of Trento. © All rights reserved. Do not copy – do not reproduce

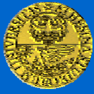

Programme

Part I

- Powder Diffraction and reciprocal lattice
- Diffraction: theoretical elements

Part II

- Applications of powder diffraction: a survey

Part III

- Introduction to line profile analysis for the study of nanocrystalline and heavily deformed materials

 © Do not copy – Do not reproduce

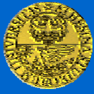

X-RAY POWDER DIFFRACTION

Most frequent applications of powder diffraction

- Crystal structure determination
  (Powder diffraction structure solution and refinement)
- Phase Identification – pure crystalline phases or mixtures
  (Search-Match procedures)
- Quantitative Phase Analysis (QPA)
- Amorphous phase analysis (radial distribution function)
- Determination of residual stress field (Residual Stress Analysis)
- Determination of preferred orientations (Texture Analysis)
- Line Profile Analysis (LPA) à *PART III*

© Do not copy – Do not reproduce

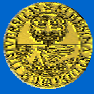

DATA PROCESSING: pattern fitting / modelling

Experimental pattern – peak identification / profile fitting

Sol-gel cerium oxide powder, 1h @ 400°C

Intensity (counts)

7000
6000
5000
4000
3000
2000
1000
0

20 40 60 80 100 120 140

2θ (degrees)

Data processing usually includes peak identification (also supported by profile fitting) and determination of peak position, intensity and width/shape.

Peak position is converted to interplanar distances by the Bragg's law: $d = \frac{l}{2\sin q}$

© Do not copy – Do not reproduce

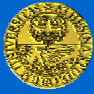

DATA PROCESSING: pattern fitting / modelling

Experimental pattern – full pattern modelling (Rietveld method, WPPM, etc.)

Sol-gel cerium oxide powder, 1h @ 400°C

P.Scardi & M. Leoni,
Acta Cryst. A 58 (2002) 190-200

Intensity (counts)

7000
6000
5000
4000
3000
2000
1000
0

20 40 60 80 100 120 140

2θ (degrees)

Data processing usually includes peak identification (also supported by profile fitting) and determination of peak position, intensity and width/shape.

Peak position is converted to interplanar distances by the Bragg's law: $d = \frac{\lambda}{2\sin\theta}$

 © Do not copy – Do not reproduce

DATA PROCESSING: peak parameters

A table of profile parameters can be obtained e.g. through peak fitting

h k l	$2q$ (degrees)	d_{hkl} (Å)	Intensity (counts)	HWHM (deg)	Shape (Lorentz fraction)
1 1 1	28.54	3.125	4.539E+03	0.7357	0.5664
2 0 0	33.06	2.707	1.168E+03	0.7587	0.3610
2 2 0	47.47	1.914	2.160E+03	0.8284	0.5609
3 1 1	56.31	1.632	1.632E+03	0.8725	0.6089
2 2 2	59.07	1.563	2.889E+02	0.8967	0.5910
4 0 0	69.37	1.354	2.783E+02	0.9015	0.7169
3 3 1	76.67	1.242	5.194E+02	1.082	0.6170
4 2 0	79.03	1.211	3.650E+02	1.041	0.8007
4 2 2	88.38	1.105	4.626E+02	1.154	0.7878
5 1 1	95.34	1.042	3.882E+02	1.223	0.7150
0 4 4	107.30	0.9567	1.444E+02	1.463	0.7269
1 3 5	114.70	0.9148	3.874E+02	1.584	0.6069
0 0 6	117.30	0.9020	2.100E+02	1.732	0.9700
0 2 6	128.40	0.8557	2.305E+02	2.024	0.4827
3 3 5	137.90	0.8254	1.518E+02	2.813	0.5211
2 2 6	141.50	0.8159	1.254E+02	2.944	0.1212

HWHM – Half Width at Half Maximum

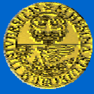

DATA PROCESSING: indexing

Lattice, unit cell and space group are obtained by indexing algorithms

2θ (degrees)	d_{hkl} (Å)
28.54	3.125
33.06	2.707
47.47	1.914
56.31	1.632
59.07	1.563
69.37	1.354
76.67	1.242
79.03	1.211
88.38	1.105
95.34	1.042
107.30	0.9567
114.70	0.9148
117.30	0.9020
128.40	0.8557
137.90	0.8254
141.50	0.8159

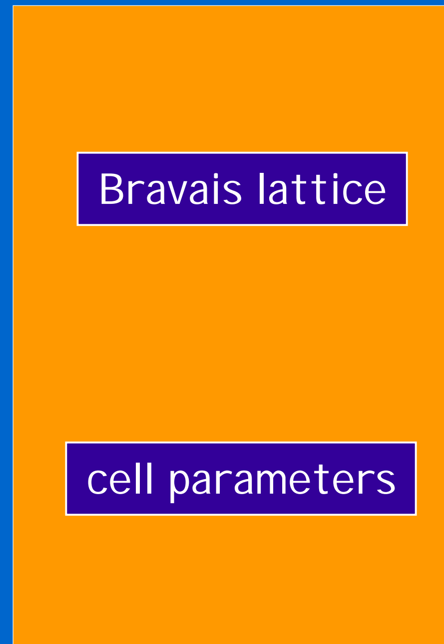

Bravais lattice

cell parameters

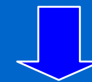

Space group
via check of systematic absences

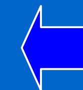

Intensity (counts)
4.539E+03
1.168E+03
2.160E+03
1.632E+03
2.889E+02
2.783E+02
5.194E+02
3.650E+02
4.626E+02
3.882E+02
1.444E+02
3.874E+02
2.100E+02
2.305E+02
1.518E+02
1.254E+02

 © Do not copy – Do not reproduce

XRD – A SURVEY OF THE MAIN APPLICATIONS

Crystal structure determination (solution) from powder diffraction patterns

© Do not copy – Do not reproduce

STRUCTURE SOLUTION: WHY POWDER ?

Structure solution of heptamethylene-1,7-bis(diphenylphosphane oxide)

Structural formula

$Ph_2P(O)(CH_2)_7P(O)Ph_2$

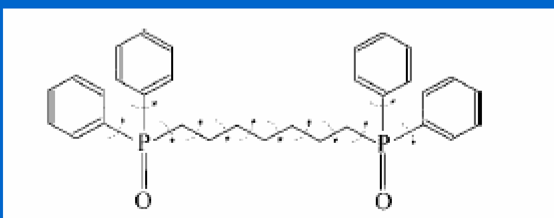

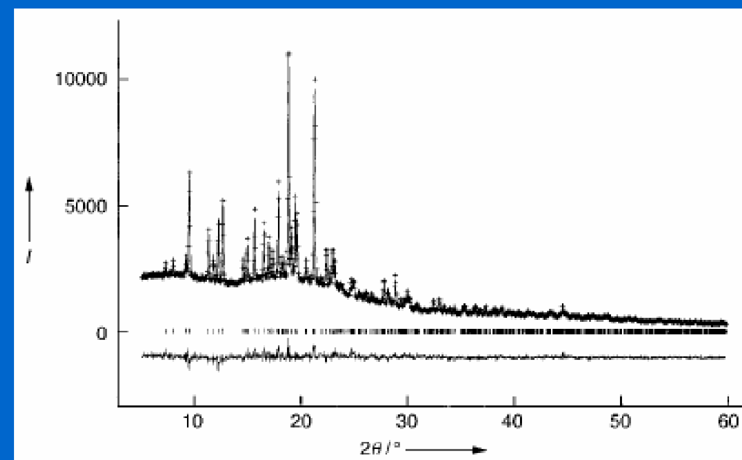

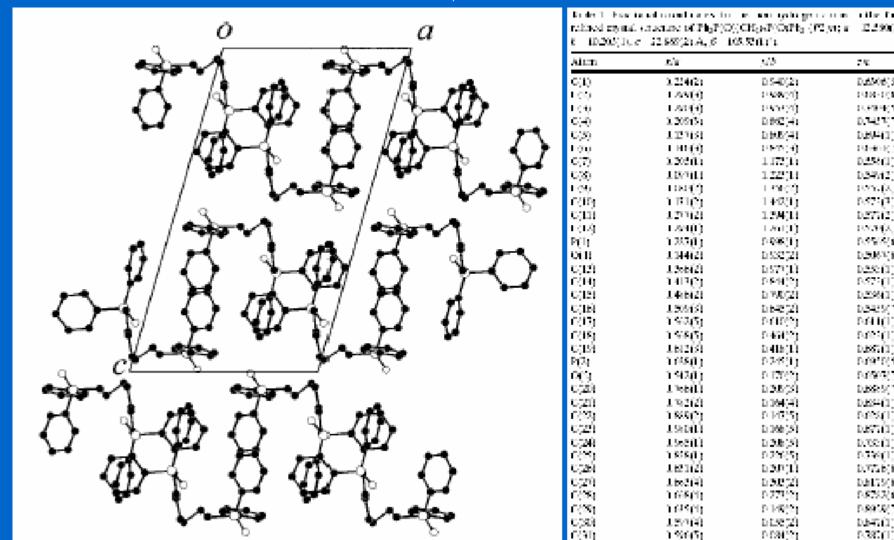

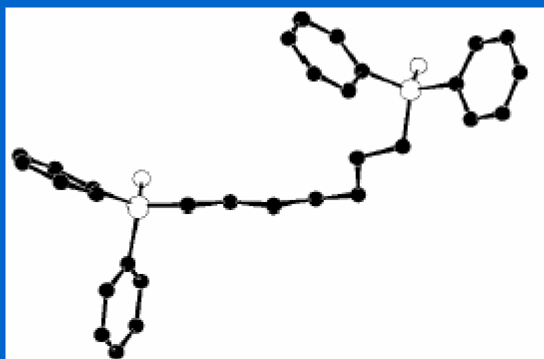

B.M. Kariuki, P. Calcagno, K. D. M. Harris, D. Philp and R.L. Johnston, Angew. Chem. Int. Ed. 1999, 38, No. 6, 831-835.

STRUCTURE SOLUTI ON: SOFTWARE

Commercial and free (shareware) software
for structure solution and refinement

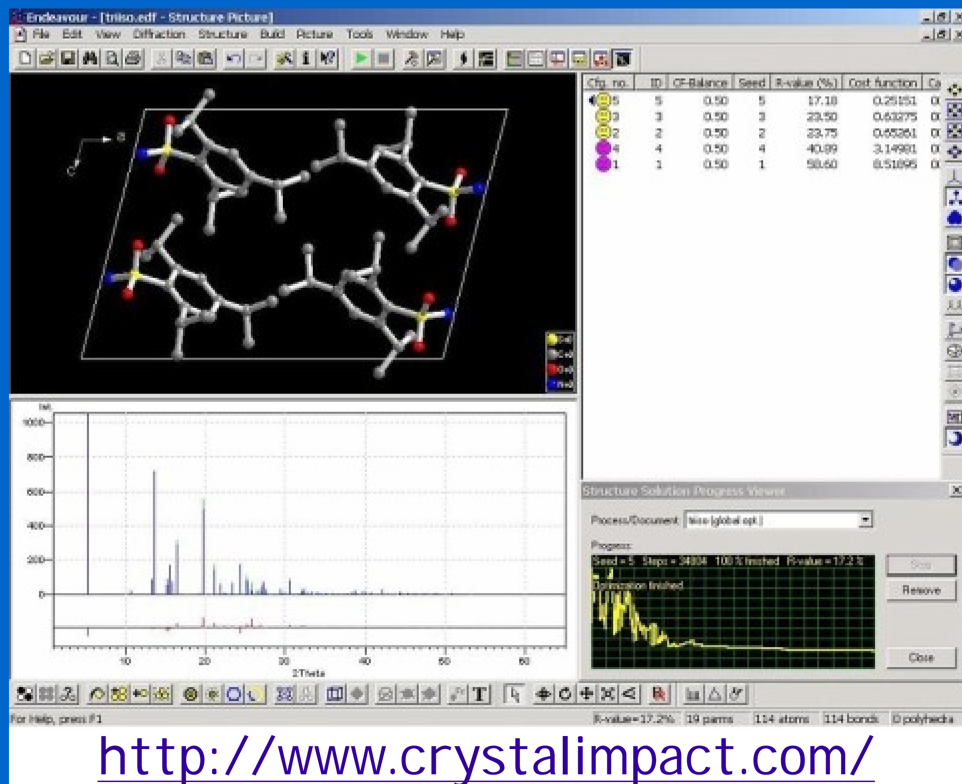

http://www.crystalimpact.com/

Structural parameters

- Cell symmetry (S.G.)
- Lattice parameters
- Atomic coordinates
- Bond angles and distances
- Site occupancy
- Thermal factors

à http://www.ccp14.ac.uk/

XRD – A SURVEY OF THE MAIN APPLICATIONS

Phase Identification
pure crystalline phases or mixtures
(Search-Match procedures)

 © Do not copy – Do not reproduce

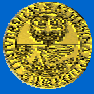

PHASE IDENTIFICATION

Phase identification is one of the first and most diffuse applications of powder diffraction, especially in industry for production, quality control and diagnostics, but also in research.

Each crystalline phase has its own pattern that can be used as a 'fingerprint'

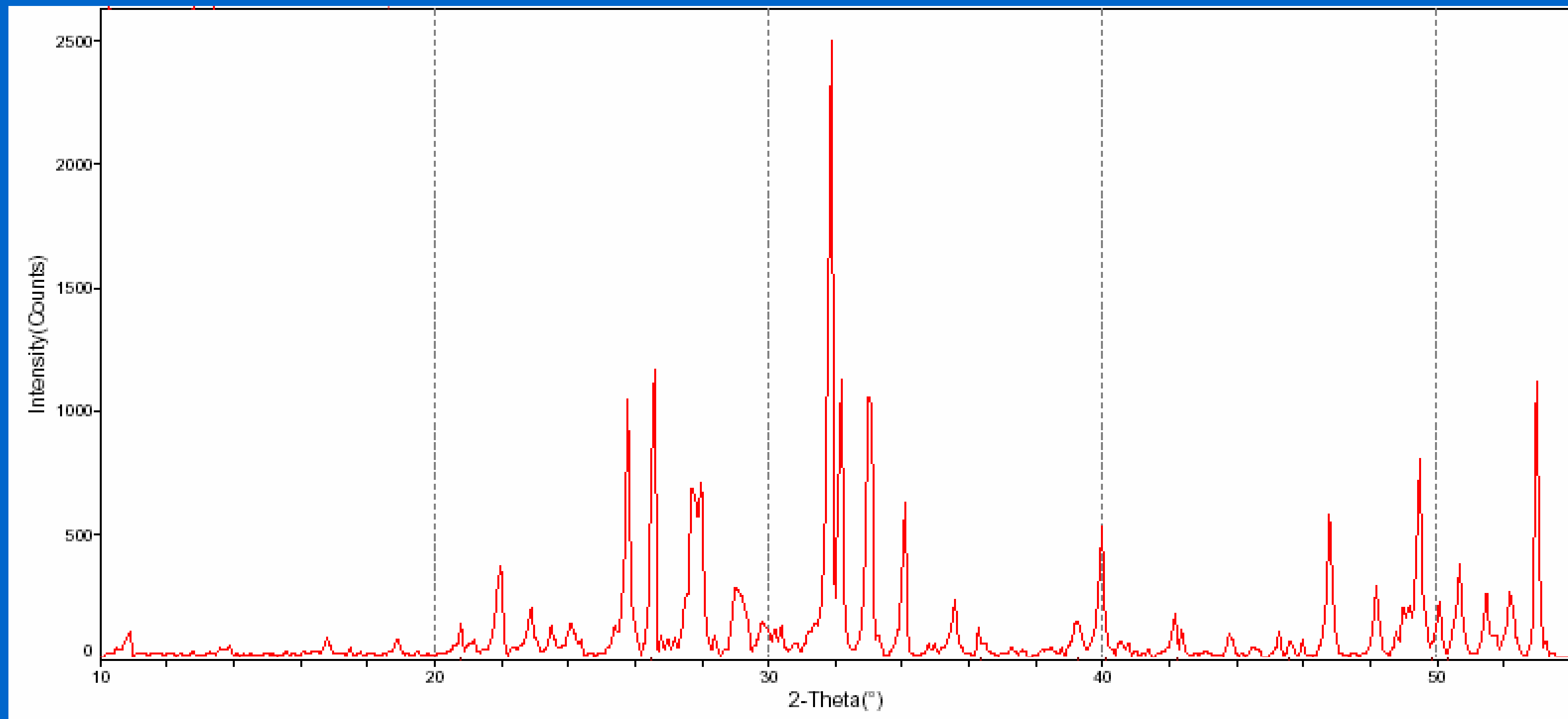

'Fingerprints' of unknown substances can be compared with those of known crystalline phases of a database à *Search-Match procedures*

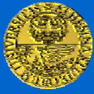

PHASE IDENTIFICATION

Manual matching of most intense lines is also possible

3.39 – 3.32 (± .02)

										File No.	I/Ic
i	3.38_9	8.58_x	3.04_9	4.11_8	3.18_8	1.69_7	2.65_6	1.88_5	$(Mg,Fe)_2Al_4Si_5O_{18}$/Cordierite, ferroan	9– 472	
	3.33_x	6.72_9	3.19_8	8.09_7	3.28_7	5.18_4	3.10_4	4.30_4	$C_{19}H_{19}N_7O_6$	29–1716	0.20
i	3.31_8	6.40_x	6.10_8	3.85_5	2.77_5	6.70_4	3.48_4	2.64_4	$C_{12}H_8Cl_6$	17–1054	
	3.38_9	6.13_x	8.66_9	3.20_9	3.29_5	9.70_3	4.57_3	3.46_3	$C_{11}H_{11}N_5 \cdot HCl$	28–1749	
i	3.34_x	5.93_2	5.19_1	3.77_1	3.65_1	3.51_1	2.94_1	1.67_1	$C_4H_8N_2O_2$	26–1863	3.30
	3.37_x	5.85_8	3.86_8	3.72_7	3.52_7	3.03_7	2.70_7	7.72_6	$C_6H_9N_3O_2 \cdot HCl$	5– 459	
*	3.31_8	5.73_x	3.43_7	3.59_6	3.19_5	4.36_4	4.19_3	3.27_2	$C_6H_5NO_2$	30–1845	1.00
	3.30_x	5.44_7	5.63_5	3.24_4	4.97_3	6.58_3	4.58_2	3.15_2	$(NH_4)_4P_2O_7$	20– 102	
	3.38_x	5.30_x	3.49_x	5.90_5	3.67_5	3.26_5	3.18_5	2.99_5	$KH_3P_2O_7$	15– 509	
	3.35_x	5.21_8	4.86_8	4.33_8	4.04_8	3.90_8	3.55_8	2.73_8	β-$C_9H_{11}NO_2$	22–1874	
i	3.40_x	5.01_9	3.09_7	4.10_4	3.00_4	4.03_3	6.74_2	3.45_2	$C_3H_6N_6$	24–1654	1.10
*	3.30_x	4.76_6	4.18_6	5.73_5	2.92_3	3.98_3	2.38_2	3.35_2	$C_8H_6O_4$	37–1919	
	3.31_x	4.71_8	3.50_5	5.56_3	3.84_3	3.03_3	7.02_2	2.30_2	$C_6H_5NO_2 \cdot HCl$	29–1827	
*	3.39_x	4.48_5	3.43_5	3.01_5	4.09_4	2.98_4	2.78_4	3.18_3	$NaHSO_4$	25– 833	
	3.34_9	4.42_x	10.1_9	1.48_9	2.56_8	1.68_8	1.28_7	1.23_7	$Al_2Si_2O_5(OH)_4 \cdot 2H_2O$/Halloysite-10A	9– 451	
i	3.40_9	4.38_x	2.88_7	5.76_4	2.61_4	4.09_4	2.76_4	1.76_3	V_2O_5/Shcherbinaite, syn	9– 387	1.60
*	3.33_x	4.30_5	2.82_5	6.08_2	4.72_2	1.71_1	3.52_1	2.15_1	$(NH_4)_2Ca_2(SO_4)_3$	22–1037	2.30
i	3.37	4.28	1.84	1.55	2.47	2.31	1.39	2.14	$AlPO_4$/Berlinite, syn	10– 423	
*	3.34_x	4.26_2	1.82_1	1.54_1	2.46_1	2.28_1	1.37_1	1.38_1	SiO_2/Quartz, low, syn	33–1161	3.60
o	3.36_x	4.23_x	3.57_7	5.27_4	3.72_4	4.04_4	3.97_3	7.19_2	$C_6H_8N_2O_3S$	30–1944	
*	3.35_x	4.22_9	3.25_7	4.43_6	3.67_5	6.22_4	2.89_4	3.55_3	[illegible]	[illegible]	
i	3.32_x	4.22_x	[illegible]	[illegible]	[illegible]	[illegible]	2.65_8	2.41_8	[illegible]	[illegible]	
i	3.35_8	3.88_x	[illegible]	[illegible]	[illegible]	[illegible]	2.32_7	1.92_5	[illegible]	[illegible]	
*	3.39_x	3.87_9	[illegible]	[illegible]	[illegible]	[illegible]	1.99_4	2.41_3	[illegible]	[illegible]	
*	3.41_9	3.84_x	3.52_9	3.26_9	3.87_7	3.03_7	2.74_3	2.37_3	$KHSO_4$/Mercallite, syn	11– 649	
*	3.31_x	3.77_8	4.22_7	3.24_7	3.29_6	2.99_5	3.47_5	2.90_5	$KAlSi_3O_8$/Orthoclase	31– 966	
*	3.36_8	3.52_x	7.69_x	6.16_5	3.84_4	3.14_1	3.79_1	3.09_1	$C_6H_4(CO)_2C_6H_4$/Hoelite, syn	28–2002	
*	3.35_x	3.50_7	5.04_6	3.56_6	4.00_5	3.15_5	5.58_4	2.48_3	$(NH_4)_2S_2O_8$	31– 69	
*	3.36_x	3.47_7	6.52_6	2.59_6	3.02_6	3.28_5	3.56_5	2.61_4	$BaAl_2Si_2O_8$/Celsian, syn	38–1450	
*	3.36_x	3.47_7	6.52_6	2.59_6	3.02_6	3.28_5	3.56_5	2.61_4	$BaAl_2Si_2O_8$/Celsian, syn	38–1450	
*	3.30_x	3.47_9	3.66_9	4.87_5	3.06_3	3.03_3	2.88_3	2.86_3	$K_2Cr_2O_7$/Lopezite, syn	27– 380	0.63
	3.33_x	3.46_6	3.79_5	3.26_5	3.01_5	2.58_5	2.91_3	2.77_3	$(K,Ba)(Si,Al)_4O_8$/Orthoclase, barian	19– 3	
*	3.38_x	3.45_7	3.44_7	2.28_6	6.30_4	2.22_3	2.75_3	5.07_3	KPO_3\Potassium metaphosphate	35– 819	
i	3.39_x	3.43_x	2.21_6	5.39_5	2.54_5	2.69_4	1.52_4	2.12_3	$Al_6Si_2O_{13}$/Mullite, syn	15– 776	
	3.39_x	3.41_9	2.31_4	2.84_3	3.82_2	2.14_2	2.03_2	2.00_2	$NaBF_4$/Ferruccite, syn	11– 671	
	3.41_9	3.39_x	2.31_4	2.84_3	3.82_2	2.14_2	2.03_2	2.00_2	$NaBF_4$/Ferruccite, syn	11– 671	
i	3.38_x	3.39_8	2.53_8	3.11_7	2.29_6	3.57_4	2.41_4	2.37_4	Gd_2S_3	20–1056	
i	3.39_8	3.38_x	2.53_8	3.11_7	2.29_6	3.57_4	2.41_4	2.37_4	Gd_2S_3	20–1056	
*	3.30_x	3.29_x	4.76_6	4.18_6	5.73_5	2.92_3	3.98_3	2.38_2	$C_8H_6O_4$	37–1919	
*	3.33_x	3.28_8	2.97_7	3.83_4	2.36_4	2.34_4	2.35_3	2.21_3	$CdSO_4$	14– 352	

Intense lines

Candidate

PDF-2

I/I_c

PHASE IDENTIFICATION

The most powerful database is the PDF (Powder Diffraction File) by the ICDD (International Centre for Diffraction Data – www.icdd.com)

PDF-2

lattice info

PDF-4

lattice info &
atomic positions
(relational database)

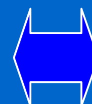

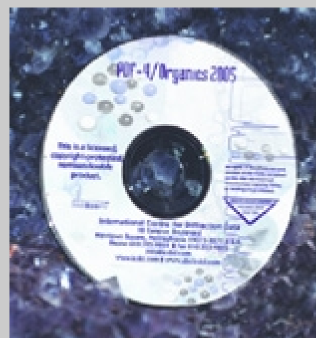

PDF-4 organics

PDF-4 minerals

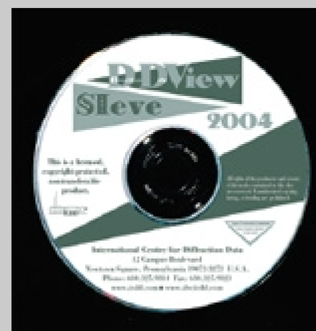

database browser

PHASE IDENTIFICATION

Each PDF entry is a card with a variety of structural information. PDF4 also includes atomic coordinate information

```
                                                                                          (14/100)
6- 2       JCPDS-ICDD Copyright (c) 2000    Radiation:          Quality: i
---------------------------------------------------------------------------------------------------
|                                                                      |  d A    | Int.|     h k l
| Ca    Mg (Si,Al) O   (OH) !6H O                                      |---------+-----+-----------
|   0.3  3       4 10     2    2                                       |         |     |
|                                                                      | 18.8    | 100 |   0  0  1
| Magnesium Aluminum Silicate Hydroxide Hydrate                        | 9.1     |  50 |   0  0  2
|                                                                      | 6.06    |  10 |   0  0  3
| Saponite-18A, glycerol                                               | 4.55    |  50 |   1  0  0
|--------------------------------------------------------------------- | 3.61    |  50 |   0  0  5
| Rad: CuKa       Lambda: 1.5418          Filter: Ni          d-sp:    |         |     |
| Cutoff:         Int: Visual             I/Icor:                      | 3.01    |  40 |   0  0  6
| Ref: Midgley, Mineral. Mag., 29 526 (1951)                           | 2.61    |  60 |   1  1  1
|                                                                      | 2.48    |  30 |
|--------------------------------------------------------------------- | 2.26    |  20 |   0  0  8
| Sys: Hexagonal            S.G.: P                                    | 2.00    |  10 |   0  0  9
| a: 5.291(7)       b:             c: 18.05(5)      A:        C: 3.4115 |         |     |
| A:                B:             C:               Z:  1     mp:      | 1.736   |  40 |   2  1  0
| Ref: Bayliss, P., Howie, R., Zussman, J., Powder Diffraction, 4 19 (1989) | 1.536 | 70 |   3  0  0
|                                                                      | 1.321   |  40 |   2  2  0
| Dx:  2.10     Dm:  2.24     SS/FOM: F(13)=1.5(0.113,76)              | 1.271   |  20 |   3  1  0
|--------------------------------------------------------------------- |         |     |
| ea:              nwB: 1.555       ey:           Sign: -   2V: 0 deg. |         |     |
| Ref: Deer, W., Howie, R., Zussman, J., Rock Forming Minerals, 3 226 (1962) |    |     |
|                                                                      |         |     |
|--------------------------------------------------------------------- |         |     |
| Color: White, reddish white                                          |         |     |
| Specimen from Lizard, Cornwall, England, UK.  CAS no.: 12173-47-6.  Glycerol |  |     |
| treated.  Smectite group, trioctahedral subgroup.  PSC: hP39.30.  Volume[CD]: | |     |
| 437.61.                                                              |         |     |
|                                                                      |         |     |
---------------------------------------------------------------------------------------------------
```

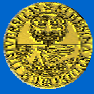

PHASE IDENTIFICATION

Line positions matched against database entries of >500000 known substances by means of Boolean search operators

A
Minerals
3544

B
Si compounds
2895

C
Strong line
at 3.34±0.02 Å
816

Information

A + B
1004

C

Subset definition

A + B + C
27

27 possible entries match the data

Matching

 © Do not copy – Do not reproduce

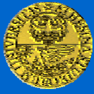

PHASE IDENTIFICATION

Intensity(Counts)

2500
2000
1500
1000
500
0

15-0876> Fluorapatite - $Ca_5(PO_4)_3F$

41-1486> Anorthite - $CaAl_2Si_2O_8$

65-0466> Quartz low - SiO_2

10 20 30 40 50

2-Theta(°)

Search-match is based on peak position / intensity

Quantitative Phase Analysis
(QPA)

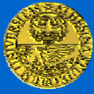

QUANTITATIVE PHASE ANALYSIS (QPA)

The pattern of a phase mixture is the WEIGHTED sum of the patterns corresponding to the constituent phases. The weight depends of the specific scattering power and absorption of each phase in the mixture.

Several techniques exists for a quantitative determination of the phase content:

- QPA with **internal standard**
- QPA with “**virtual standard**” (RIR method)
- QPA via the **Rietveld method**

© Do not copy – Do not reproduce

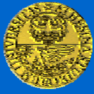

QUANTITATIVE PHASE ANALYSIS (QPA)

Mass absorption coefficient for a mixture if *n* phases:

$$(\mu/\rho)_m = w_1(\mu/\rho)_1 + w_2(\mu/\rho)_2 + \ldots + w_n(\mu/\rho)_n = \sum_{i=1}^{n} w_i(\mu/\rho)_i$$

Intensity for the *i*-th reflection in a single-phase pattern

$$I_i = k_i \frac{|F_i|^2}{\mu_i} LP = \frac{k_i'}{\mu_i}$$

Intensity for the *i*-th reflection and *j*-th phase in a multi-phase pattern

$$I_{i,j} = \frac{k_{i,j}' v_j}{(\mu/\rho)_m \rho_m} = \frac{k_{i,j}' v_j}{\mu_m}$$

volume fraction of j-th phase

linear absorption coefficient of the phase mixture

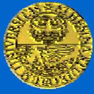

QUANTITATIVE PHASE ANALYSIS (QPA)

We can conveniently introduce the weight fractions

$$\mathbf{r}_j = \frac{w_j}{v_j}\mathbf{r}_m \qquad I_{i,j} = \frac{k'_{i,j} v_j}{\mathbf{m}_m} = \frac{k'_{i,j} w_j}{\mathbf{r}_j \left(\mathbf{m}/\mathbf{r}\right)_m} = \frac{k''_{i,j} w_j}{\left(\mathbf{m}/\mathbf{r}\right)_m}$$

mass absorption coefficient of the phase mixture

For two phases, the formula reduces to:

$$I_{i,1} = \frac{k''_{i,1} w_1}{\left(\mathbf{m}/\mathbf{r}\right)_m} = \frac{k''_{i,1} w_1}{\left[\left(\mathbf{m}/\mathbf{r}\right)_1 - \left(\mathbf{m}/\mathbf{r}\right)_2\right] w_1 + \left(\mathbf{m}/\mathbf{r}\right)_2}$$

$$w_1 = 1 - w_2,\; v_1 = 1 - v_2$$

The mass absorption coefficient is however unknown!

© Do not copy – Do not reproduce

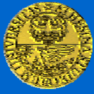

QUANTITATIVE PHASE ANALYSIS

(a) Quartz (1) –Berillia (2) : $(m/r)_1 > (m/r)_2$, $(m/r)_1 = 34.9$, $(m/r)_2 = 8.6$ [cm^2/g]

(b) Quartz (1) –Cristobalite (2) : $(m/r)_1 = (m/r)_2 = 34.9$ [cm^2/g]

(c) Quartz (1) –Sylvite (2) : $(m/r)_1 < (m/r)_2$, $(m/r)_1 = 34.9$, $(m/r)_2 = 124.0$ [cm^2/g]

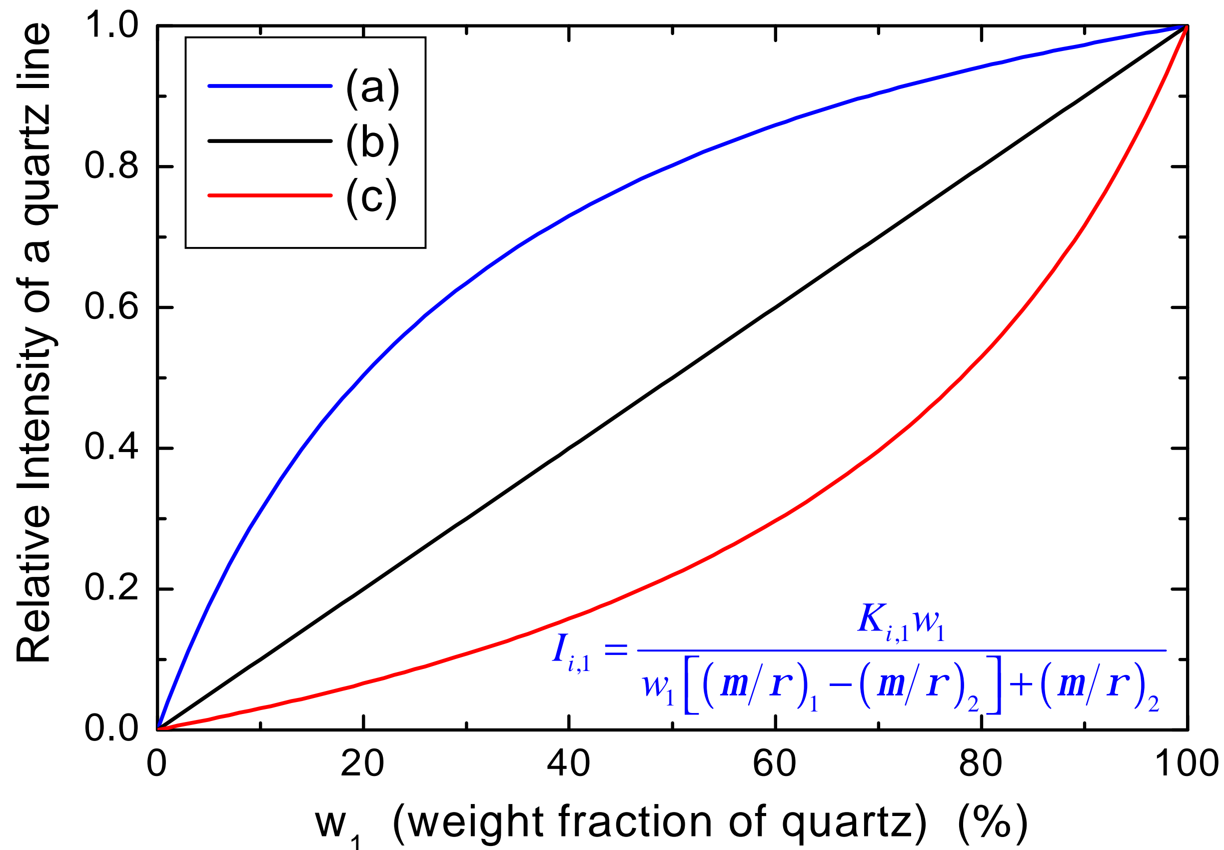

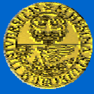

QUANTITATIVE PHASE ANALYSIS (QPA)

The problem of the (unknown) mass absorption coefficient can be solved by adding a known amount of a standard material.

Assuming that the amount of phase to be determined is w_j , the known amount of an extra phase (spiking) is w_s. By effect of the extra phase:

$$w'_j = (1 - w_s)w_j$$

then the ratio of the intensities of two peaks for the *j* and *s* phases reads:

$$\frac{I'_{i,j}}{I_{l,s}} = \frac{k_{i,j} w'_j}{k_{l,s} w_s} = f_{j,s} \frac{w'_j}{w_s} = f_{j,s} \frac{w_j (1 - w_s)}{w_s}$$

from which, if the structure of the phases (and therefore $f_{j,s}$) is known:

$$w_j = \frac{I_{i,j}}{I_{r,s}} \cdot \frac{w_s}{f_{j,s}(1 - w_s)}$$

© Do not copy – Do not reproduce

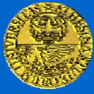

QUANTITATIVE PHASE ANALYSIS (QPA)

There is a possible elegant and effective alternative to use an internal standard. For a 1:1 mixture of the given phase and a corundum standard $f_{j,s}$ is:

$$f_{j,s} = \frac{I_{i,j}}{I_{l,c}} \cdot \frac{w_c}{w_j\left(1-w_c\right)} = 2\frac{I_{i,j}}{I_{l,c}}$$

The ratio between the most intense peaks of the given phase and of corundum is defined as Reference Intensity Ratio (RIR):

$$RIR_{j,corundum} = I_j / I_c = \frac{I_{i,j}}{I_{l,c}} \frac{I_{l,c}^{rel}}{I_{i,j}^{rel}} \frac{w_c}{w_j}$$

For a peak i and phase j with relative intensity $I_{i,j}^{rel}$ we have:

$$w_j = \frac{I_{i,j} / I_{i,j}^{rel}}{I_j / I_c} \left[\sum_{k=1}^{n} \frac{I_{l,k} / I_{l,k}^{rel}}{I_k / I_c} \right]^{-1}$$

If the RIR is known for all the phases in a mixture (from the PDF database), the above expression allows a QPA with no standard addition

QUANTITATIVE PHASE ANALYSIS (QPA)

The RIR (also called I/Ic) is given in the PDF for many phases

3.39 – 3.32 (± .02)

										File No.	I/Ic
i	3.38_9	8.58_x	3.04_9	4.11_8	3.18_8	1.69_7	2.65_6	1.88_5	$(Mg,Fe)_2Al_4Si_5O_{18}$/Cordierite, ferroan	9– 472	
	3.33_x	6.72_9	3.19_8	8.09_7	3.28_7	5.18_4	3.10_4	4.30_4	$C_{19}H_{19}N_7O_6$	29–1716	0.20
i	3.31_8	6.40_x	6.10_8	3.85_5	2.77_5	6.70_4	3.48_4	2.64_4	$C_{12}H_6Cl_6$	17–1054	
	3.38_9	6.13_x	8.66_9	3.20_9	3.29_5	9.70_3	4.57_3	3.46_3	$C_{11}H_{11}N_5 \cdot HCl$	28–1749	
i	3.34_x	5.93_2	5.19_1	3.77_1	3.65_1	3.51_1	2.94_1	1.67_1	$C_4H_8N_2O_2$	26–1863	3.30
	3.37_x	5.85_8	3.86_8	3.72_7	3.52_7	3.03_7	2.70_7	7.72_6	$C_6H_9N_3O_2 \cdot HCl$	5– 459	
*	3.31_8	5.73_x	3.43_7	3.59_6	3.19_5	4.36_4	4.19_3	3.27_2	$C_6H_5NO_2$	30–1845	1.00
	3.30_x	5.44_7	5.63_5	3.24_4	4.97_3	6.58_3	4.58_2	3.15_2	$(NH_4)_4P_2O_7$	20– 102	
	3.38_x	5.30_x	3.49_x	5.90_5	3.67_5	3.26_5	3.18_5	2.99_5	$KH_3P_2O_7$	15– 509	
	3.35_x	5.21_8	4.86_8	4.33_8	4.04_8	3.90_8	3.55_8	2.73_8	β-$C_9H_{11}NO_2$	22–1874	
i	3.40_x	5.01_9	3.09_7	4.10_4	3.00_4	4.03_3	6.74_2	3.45_2	$C_3H_6N_6$	24–1654	1.10
*	3.30_x	4.76_6	4.18_6	5.73_5	2.92_3	3.98_3	2.38_2	3.35_2	$C_8H_6O_4$	37–1919	
	3.31_x	4.71_8	3.50_5	5.56_3	3.84_3	3.03_3	7.02_2	2.30_2	$C_6H_5NO_2 \cdot HCl$	29–1827	
*	3.39_x	4.48_5	3.43_5	3.01_5	4.09_4	2.98_4	2.78_4	3.18_3	$NaHSO_4$	25– 833	
	3.34_9	4.42_x	10.1_9	1.48_9	2.56_8	1.68_8	1.28_7	1.23_7	$Al_2Si_2O_5(OH)_4 \cdot 2H_2O$/Halloysite-10A	9– 451	
i	3.40_9	4.38_x	2.88_7	5.76_4	2.61_4	4.09_4	2.76_4	1.76_3	V_2O_5/Shcherbinaite, syn	9– 387	1.60
*	3.33_x	4.30_5	2.82_5	6.08_2	4.72_2	1.71_1	3.52_1	2.15_1	$(NH_4)_2Ca_2(SO_4)_3$	22–1037	2.30
i	3.37_x	4.28_3	1.84_2	1.55_1	2.47_1	2.31_1	1.39_1	2.14_1	$AlPO_4$/Berlinite, syn	10– 423	
*	3.34_x	4.26_2	1.82_1	1.54_1	2.46_1	2.28_1	1.37_1	1.38_1	SiO_2/Quartz, low, syn	33–1161	3.60
o	3.36_x	4.23_x	3.57_7	5.27_4	3.72_4	4.04_4	3.97_3	7.19_2	$C_6H_8N_2O_3S$	30–1944	
*	3.35_x	4.22_9	3.25_7	4.43_6	3.67_5	6.22_4	2.89_4	3.55_3	$C_6H_4N_2O_4$	37–1915	
i	3.32_x	4.22_x	5.28_8	4.97_8	3.52_8	3.48_8	2.65_8	2.41_8	$C_6H_{14}N_4O_2 \cdot HCl$	25–1541	
i	3.35_8	3.88_x	3.73_8	3.54_8	2.91_7	2.52_7	2.32_7	1.92_5	$C_5H_9NO_4 \cdot HCl$	25–1925	
*	3.39_x	3.87_9	3.29_8	2.36_6	3.01_5	2.04_4	1.99_4	2.41_3	$HgSO_4$	31– 867	
*	3.41_9	3.84_x	3.52_9	3.26_9	3.87_7	3.03_7	2.74_3	2.37_3	$KHSO_4$/Mercallite, syn	11– 649	
*	3.31_x	3.77_8	4.22_7	3.24_7	3.29_6	2.99_5	3.47_5	2.90_3	$KAlSi_3O_8$/Orthoclase	31– 966	
*	3.36_8	3.52_x	7.69_x	6.16_5	3.84_4	3.14_1	3.79_1	3.09_1	$C_6H_4(CO)_2C_6H_4$/Hoelite, syn	28–2002	
*	3.35_x	3.50_7	5.04_6	3.56_6	4.00_5	3.15_5	5.58_4	2.48_3	$(NH_4)_2S_2O_8$	31– 69	
*	3.36_x	3.47_7	6.52_6	2.59_6	3.02_6	3.28_5	3.56_5	2.61_4	$BaAl_2Si_2O_8$/Celsian, syn	38–1450	
*	3.36_x	3.47_7	6.52_6	2.59_6	3.02_6	3.28_5	3.56_5	2.61_4	$BaAl_2Si_2O_8$/Celsian, syn	38–1450	
*	3.30_x	3.47_9	3.66_9	4.87_5	3.06_3	3.03_3	2.88_3	2.86_3	$K_2Cr_2O_7$/Lopezite, syn	27– 380	0.63
	3.33_x	3.46_6	3.79_5	3.26_5	3.01_5	2.58_5	2.91_3	2.77_3	$(K,Ba)(Si,Al)_4O_8$/Orthoclase, barian	19– 3	
*	3.38_x	3.45_7	3.44_7	2.28_6	6.30_4	2.22_3	2.75_3	5.07_3	KPO_3\Potassium metaphosphate	35– 819	
i	3.39_x	3.43_x	2.21_6	5.39_5	2.54_5	2.69_4	1.52_4	2.12_3	$Al_6Si_2O_{13}$/Mullite, syn	15– 776	
	3.39_x	3.41_9	2.31_4	2.84_3	3.82_2	2.14_2	2.03_2	2.00_2	$NaBF_4$/Ferruccite, syn	11– 671	
	3.41_9	3.39_x	2.31_4	2.84_3	3.82_2	2.14_2	2.03_2	2.00_2	$NaBF_4$/Ferruccite, syn	11– 671	
i	3.38_x	3.39_8	2.53_8	3.11_7	2.29_6	3.57_4	2.41_4	2.37_4	Gd_2S_3	20–1056	
i	3.39_8	3.38_x	2.53_8	3.11_7	2.29_6	3.57_4	2.41_4	2.37_4	Gd_2S_3	20–1056	
*	3.30_x	3.29_x	4.76_6	4.18_6	5.73_5	2.92_3	3.98_3	2.38_2	$C_8H_6O_4$	37–1919	
*	3.33_x	3.28_8	2.97_7	3.83_4	2.36_4	2.34_4	2.35_3	2.21_3	$CdSO_4$	14– 352	

I/I c

© Do not copy – Do not reproduce

The RIETVELD method

© Do not copy – Do not reproduce

THE RIETVELD METHOD

Definition - R.A. Young, The Rietveld Method, OUP 1993, page 2:

In the Rietveld method the least-squares refinements are carried out until the best fit is obtained between the entire observed powder diffraction pattern taken as a whole and the entire calculated pattern based on the simultaneously refined models for the crystal structure(s), diffraction optics effects, intrumental factors, and other specimen characteristics

The Rietveld method is based on a minimization procedure (Nonlinear Least Squares refinement) of the residual:

$$S_y = \sum_i w_i \left(y_i - y_{ci} \right)^2$$

weight

observed

calculated

© Do not copy – Do not reproduce

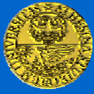

THE RIETVELD METHOD

Intensity of the i-th point in the pattern

$$y_{ci} = S \sum_k L_k \left|F_k\right|^2 f\left(2\theta_i - 2\theta_k\right) P_k A + y_{bi}$$

Scale factor

Structure factor

Profile function

Background term

Using the normalization condition: $\sum_k x_k = 1$ (not obvious !!)

it is possible to calculate the weight fraction x_j of the phase *j* in a polyphasic mixture as:

$$x_j = \frac{S_j \rho_j v_j}{\sum_l S_l \rho_l v_l}$$

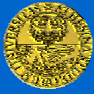

THE RIETVELD METHOD

Statistical indices

$$R_F = \frac{\sum |(I_K(\text{'obs'}))^{1/2} - (I_K(\text{calc})^{1/2})|}{\sum (I_K(\text{'obs'}))^{1/2}} \quad \text{('R-structure factor')}$$

$$R_B = \frac{\sum |I_K(\text{'obs'}) - I_K(\text{calc})|}{\sum I_K(\text{'obs'})} \quad \text{('R-Bragg factor')}$$

$$R_p = \frac{\sum |y_i(\text{obs}) - y_i(\text{calc})|}{\sum y_i(\text{obs})} \quad \text{('R-pattern')}$$

$$R_{wp} = \left\{ \frac{\sum w_i (y_i(\text{obs}) - y_i(\text{calc}))^2}{\sum w_i (y_i(\text{obs}))^2} \right\}^{1/2} \quad \text{('R-weighted pattern')}$$

Here I_K is the intensity assigned to the Kth Bragg reflection at the end of the refinement cycles. In the expressions for R_F and R_B the 'obs' (for observed) is put in quotation marks because the Bragg intensity, I_K, is rarely observed directly; instead the I_K values are obtained from programmatic allocation of the total observed intensity in a 'scramble' of overlapped reflections to the individual reflections, according to the ratios of those reflection intensities in the calculated pattern.

The '*Goodness-of-fit*' indicator, S, is

$$S = [S_y/(N - P)]^{1/2} = R_{wp}/R_e$$

where

$$R_e = \text{'R-expected'} = [(N - P)/\sum w_i y_{oi}^2]^{1/2}.$$

The *Durbin Watson statistic*, 'd', is

$$\text{'}d\text{'} = \sum_{i=2}^{N} (\Delta y_i - \Delta y_{i-1})^2 \Big/ \sum_{i=1}^{N} \Delta y_i^2$$

where

$$\Delta y_i = y_{oi} - y_{ci}.$$

THE RIETVELD METHOD

The Rietveld method was originally conceived for structure *refinement* …

Structural parameters

- Cell symmetry (S.G.)
- Lattice parameters
- Atomic coordinates
- Bond angles and distances
- Site occupancy
- Thermal factors

à http://www.ccp14.ac.uk/

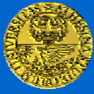

RIETVELD-BASED QPA

… but is very convenient for *QPA*. Example: zirconia polymorphs in Partially-Stabilised Zirconia TBCs (Thermal Barrier Coatings) used for turbine blades

Tetragonal 94.0 wt%
Monoclinic 6.0 wt%

M (-111)
M (111)

Intensity (counts)

2θ (degrees)

© Do not copy – Do not reproduce

Amorphous phase analysis
(radial distribution function)

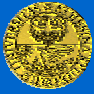

AMORPHOUS PHASE ANALYSIS

The long-range order typical of crystalline structures is absent in amorphous materials. However, a certain degree of short-range order is always present.

Diffraction can be used to measure the ***radial distribution function***, i.e., the probability distribution to find an atom at a distance between *r* and *r+dr* taken from a reference atom.

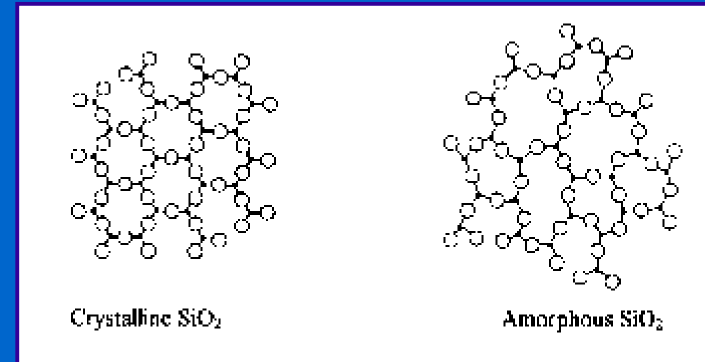

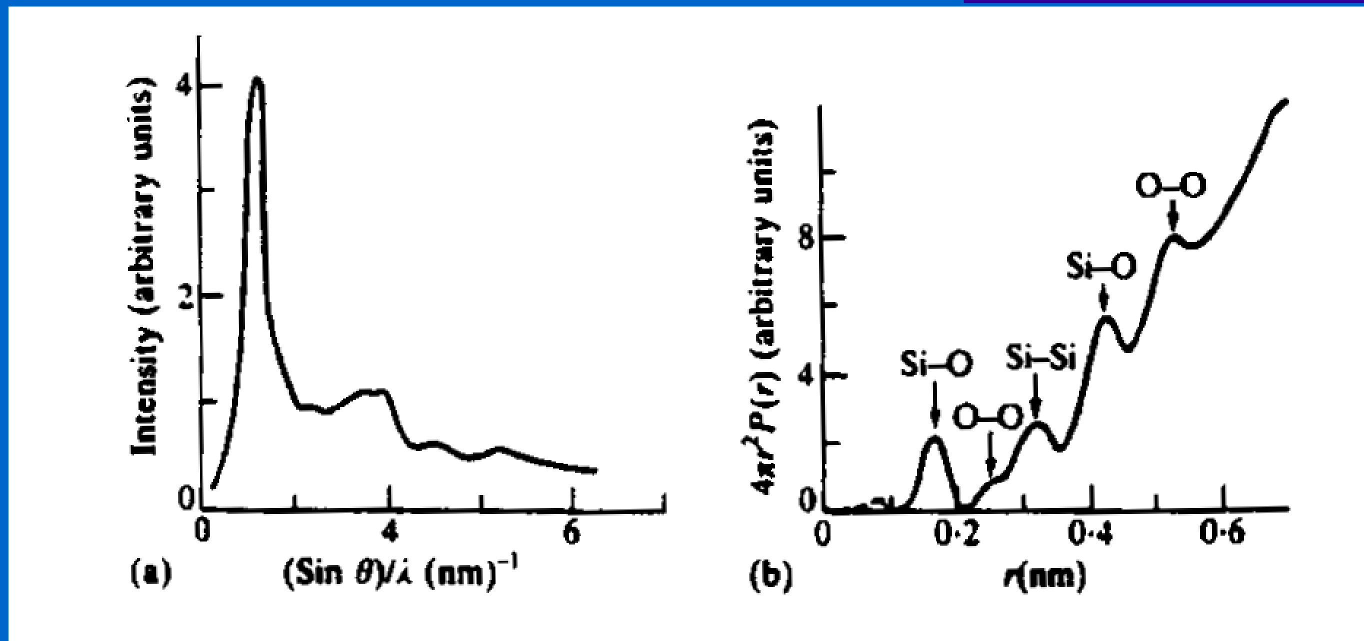

 © Do not copy – Do not reproduce

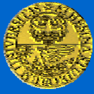

AMORPHOUS PHASE ANALYSIS

Mixture of (crystalline) corundum and amorphous silica

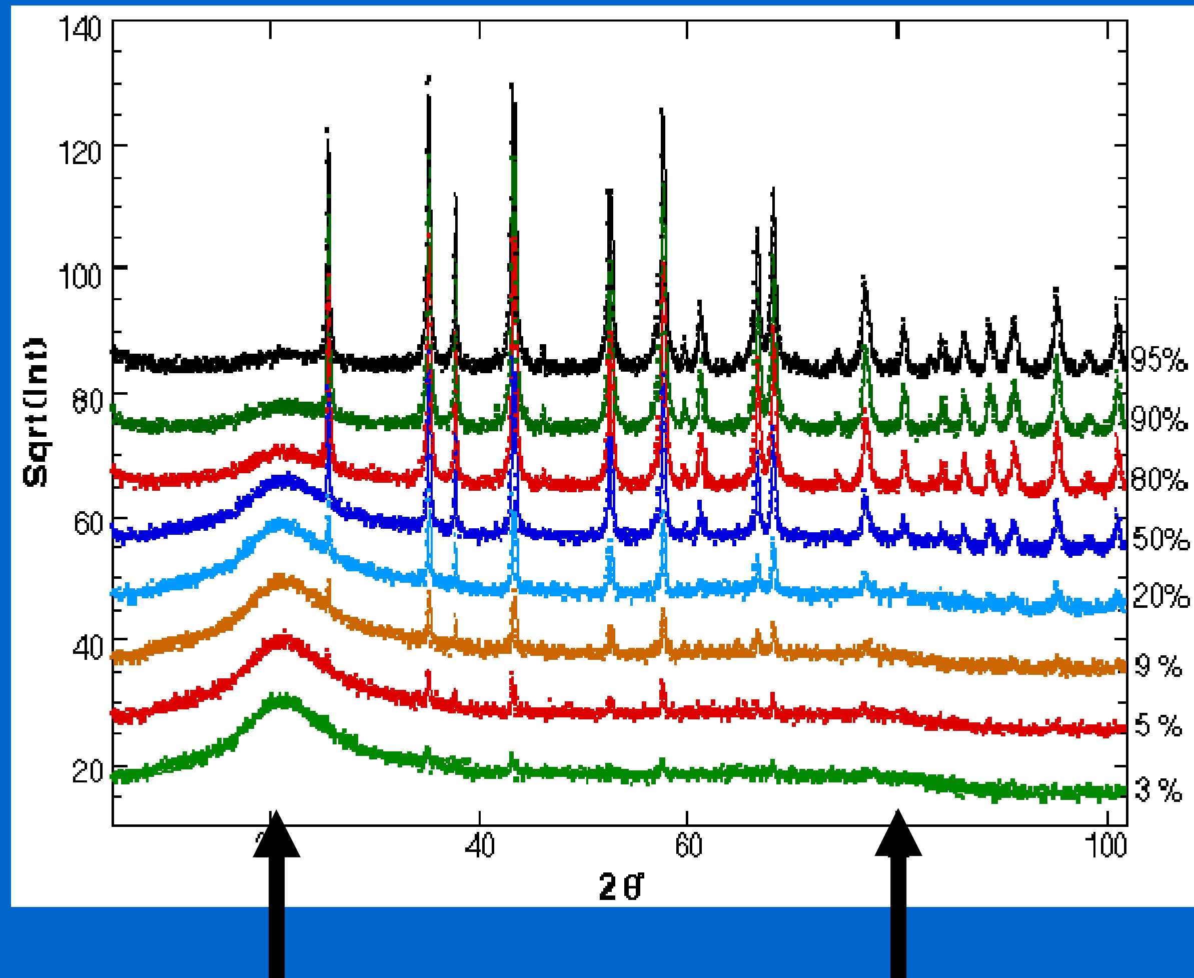

amorphous bands typical of the glass

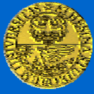

AMORPHOUS PHASE ANALYSIS

Modelling of amorphous and crystalline peaks provides the **fraction of amorphous phase** in mixtures.

Diffraction can also measure the **degree of crystallinity** in partly-crystalline materials, like polymers or glass-ceramics.

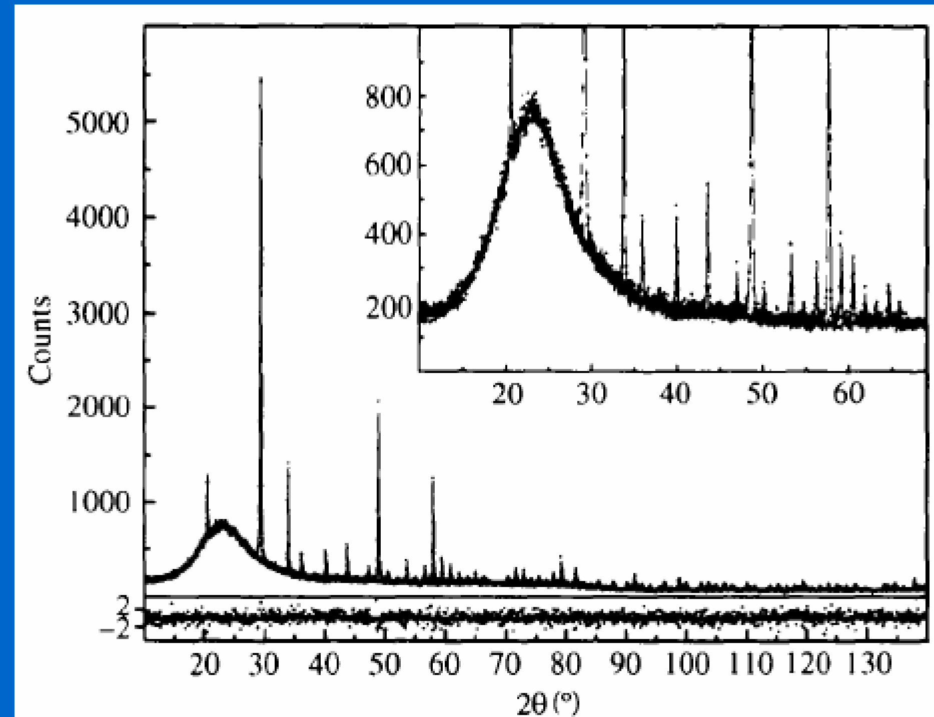

Fig. 1. Rietveld analysis of sample *C* (Y_2O_3/amorphous silica with weight ratio 10:90) with air scattering subtracted. In the inset, which shows an enlargement, the experimental noise of the amorphous scattering used in the fitting is evident. At the bottom, the weighted residuals are reported. Because of the noise in the amorphous pattern, the normalized residuals are defined as $\Delta Y_i(\text{weighted}) = (Y_{oi} - Y_{ci})/[Y_{oi} + (K^{am})^2 Y^{am}]^{1/2}$ and consequently the goodness of fit is $S^2 = \{\sum[\Delta Y_i(\text{weighted})]^2\}/(N - P) = 1.3$.

P. Riello, P. Canton, G. Fagherazzi, J. Appl. Cryst. 1998, 31, 78-82.

XRD – A SURVEY OF THE MAIN APPLICATIONS

Residual stress analysis

© Do not copy – Do not reproduce

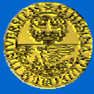

Why residual stresses?

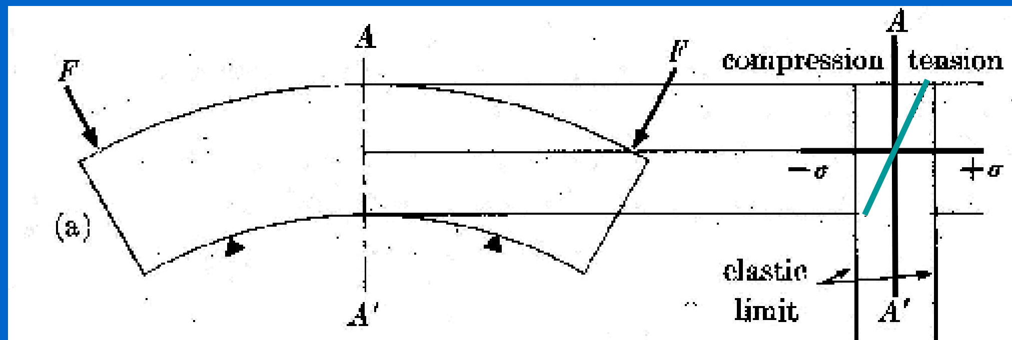

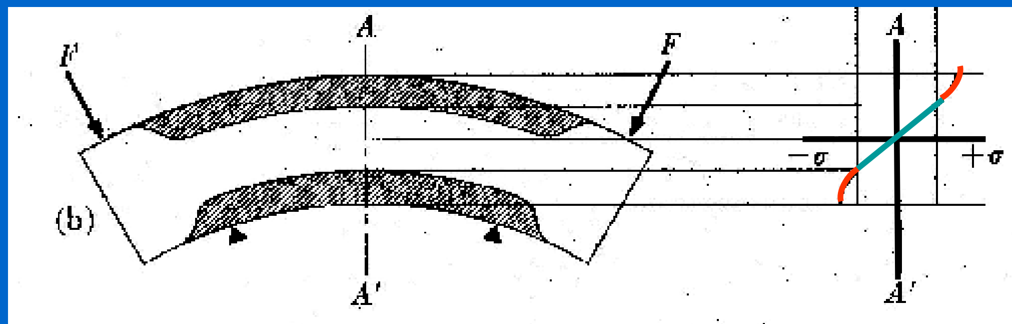

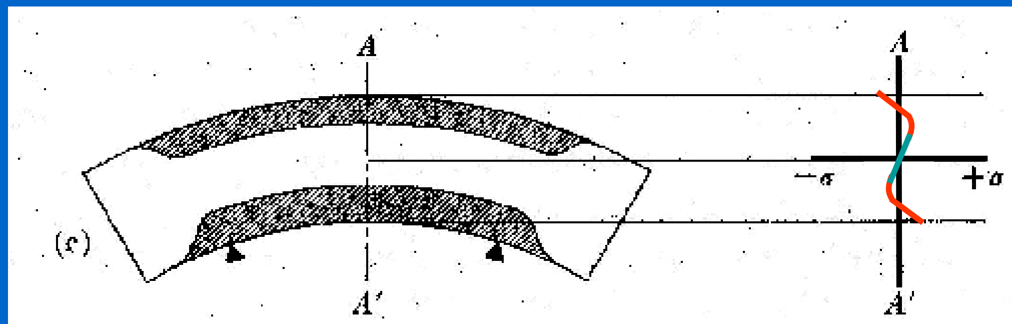

Example: residual stress by plastic flow in bending:

(a) loaded below elastic limit

(b) loaded above elastic limit

(c) unloaded

Shaded regions have been plastically deformed

Source: B.D. Cullity "Elements of X-ray diffraction" II Edition. Addison-Wesley. Reading (1978)

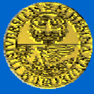

RESIDUAL STRESS ANALYSIS

Crystalline domains can be used as strain gauges

grain deformation

$$e = \frac{\Delta l}{l}$$

lattice deformation

$$e = \frac{\Delta d}{d}$$

The deformation is measured along different directions, by tilting the sample.
The in-plane strain is obtained by measuring *d* along off-plane directions.

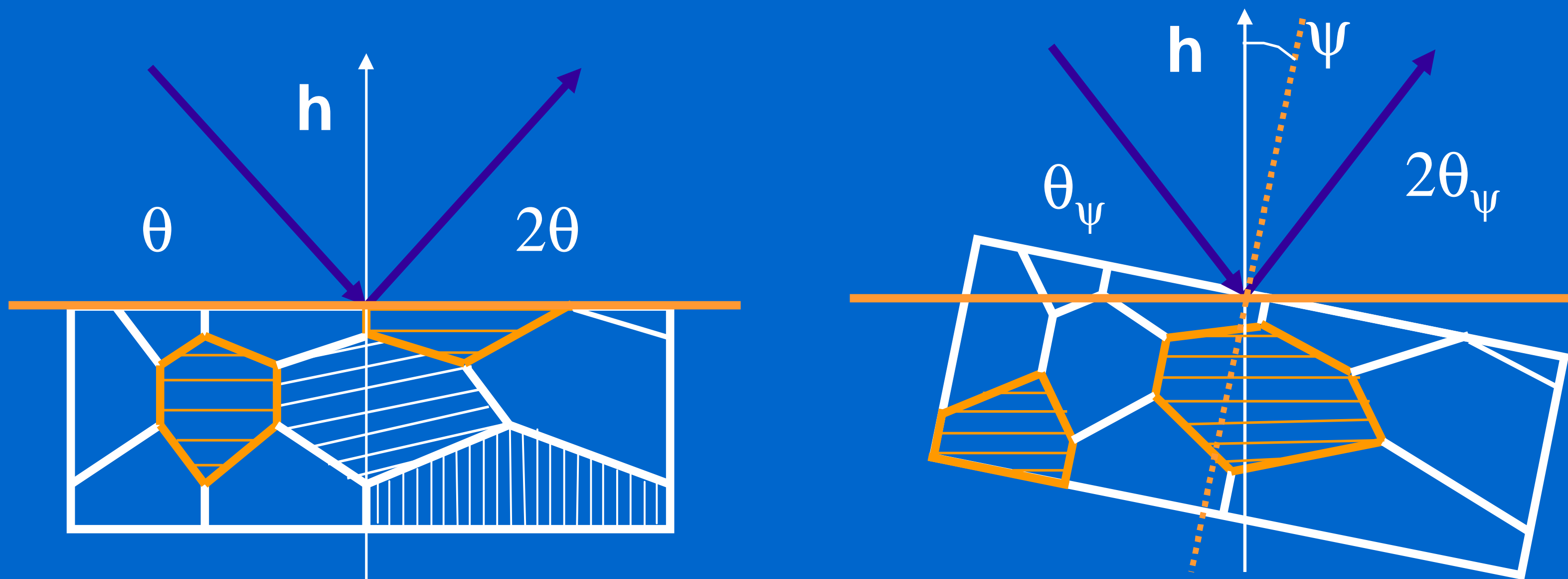

 © Do not copy – Do not reproduce

RESIDUAL STRESS ANALYSIS

We need therefore additional movements for the specimen, with respect to the traditional Bragg-Brentano (powder) setup

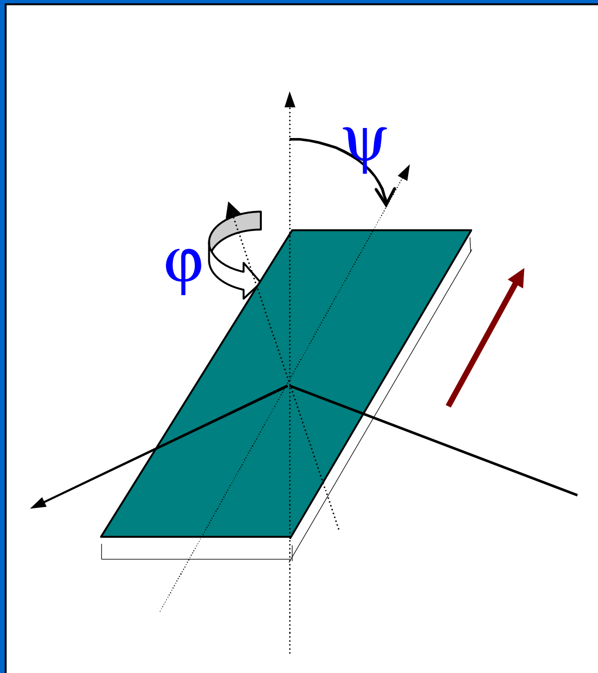

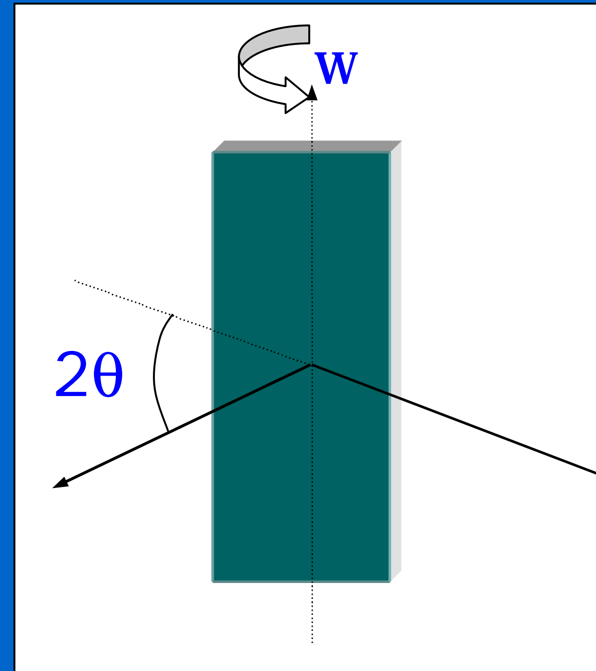

The sample should be tilted/rotated along its three axes.

RESIDUAL STRESS ANALYSIS

specimen

ϕ

ψ

source

$\pi-2\theta$

detector

© Do not copy – Do not reproduce

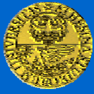

RESIDUAL STRESS ANALYSIS

If the stress field is plane and rotationally symmetric:

$\sigma_{11}=\sigma_{22}=\sigma_{||}, \ \sigma_{12}=\sigma_{13}=\sigma_{23}=\sigma_{33}=0$

and if no gradient and no texture are present, then:

$$< e_{y}^{hkl} > = \left(2S_1^{hkl} + ½S_2^{hkl}\sin^2 y\right) s_P^S$$

"$\sin^2\psi$ formula"

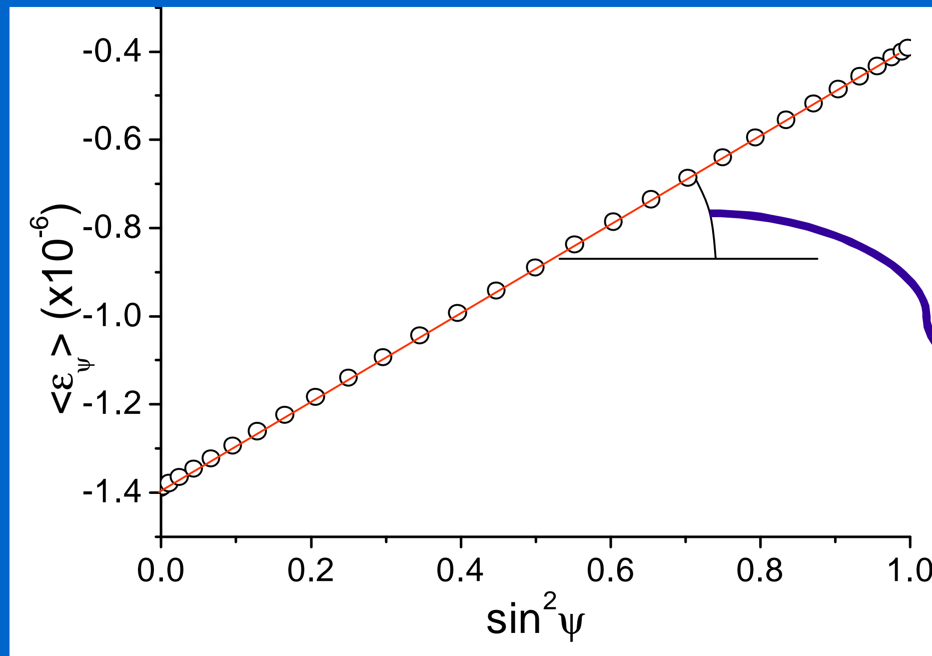

$S_1^{hkl}, \ ½S_2^{hkl}$

X-ray elastic constants (XECs)

slope related to the average *in-plane* stress

Analysis of the preferred orientation

(Texture analysis)

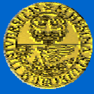

TEXTURE ANALYSIS

A 'true' powder has randomly oriented crystalline domains.
The diffracted intensity does not depend on the probing direction.

for any *hkl*

random orientation

© Do not copy – Do not reproduce

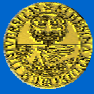

TEXTURE ANALYSIS

If the grain (crystal) orientation is not random, the diffracted signal depends on the incident angle.

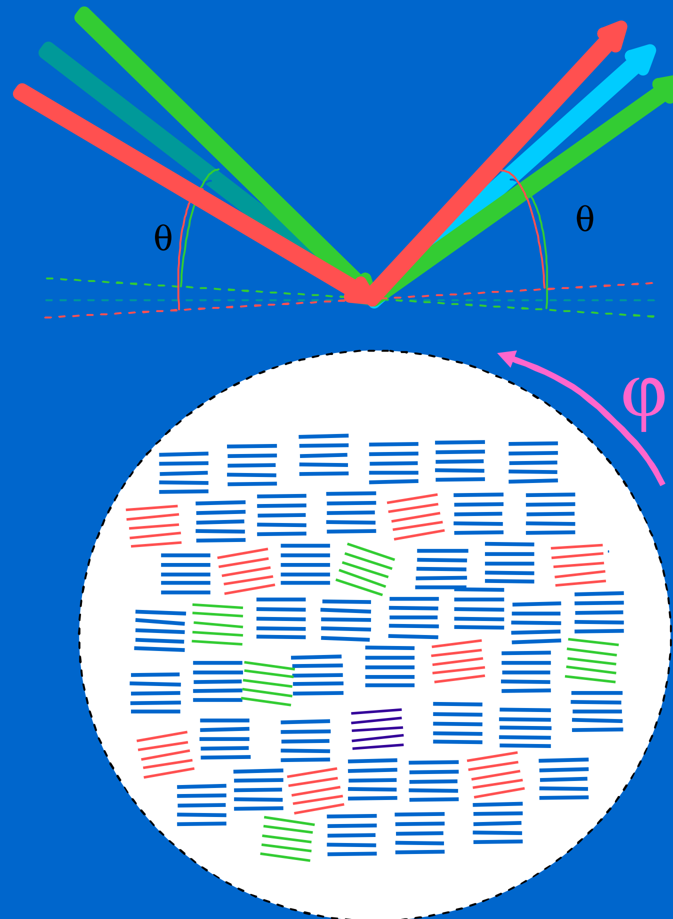

preferred orientation

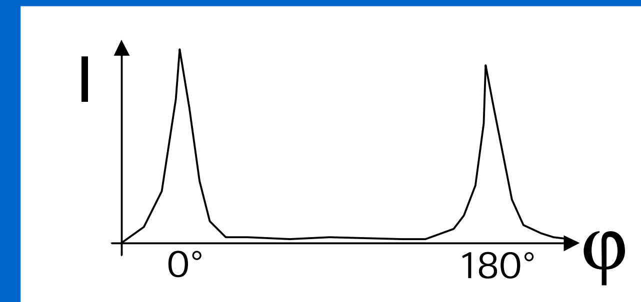

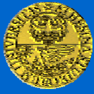

TEXTURE ANALYSIS

The information can be reported on suitable maps: pole figures.
The stereographic projection is adopted

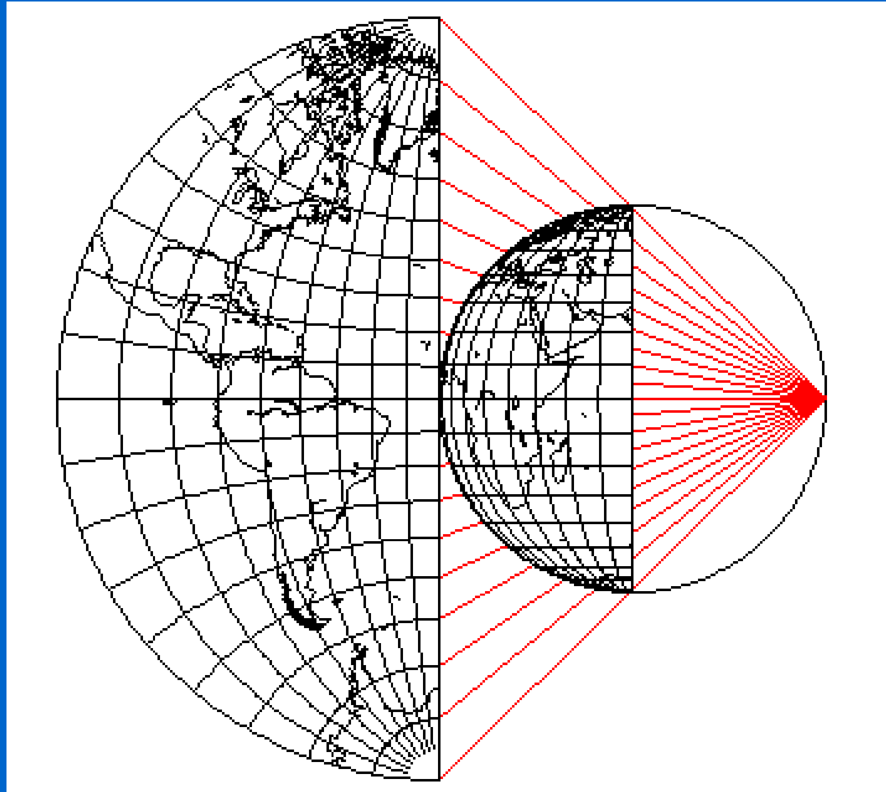

Two angles are used in the projection

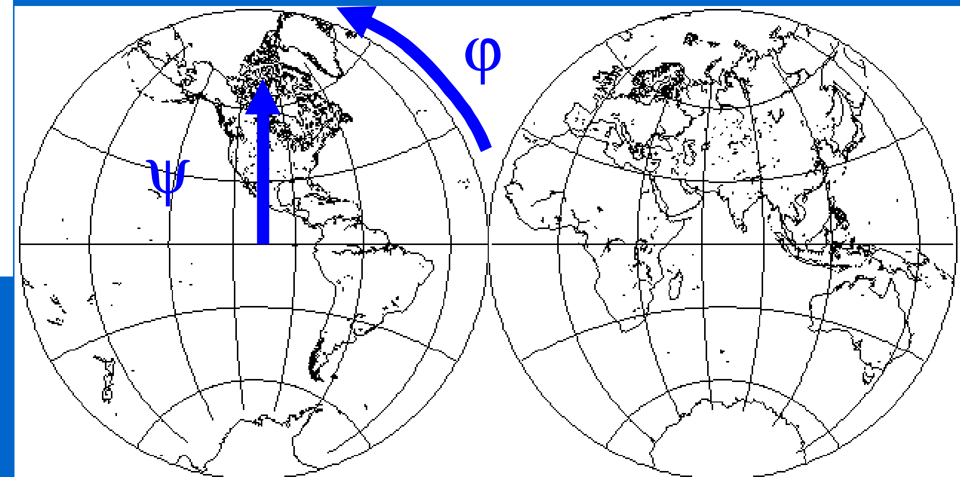

© Do not copy – Do not reproduce

TEXTURE ANALYSIS

Eulerian cradle for stress/texture measurement: laboratory instrum.

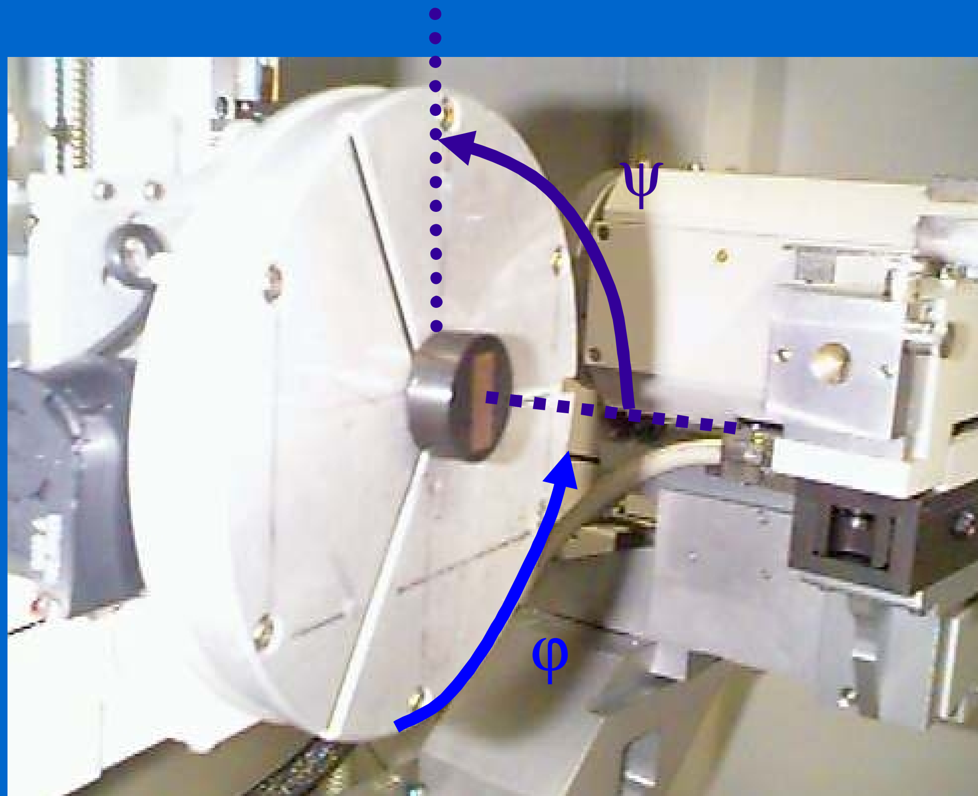

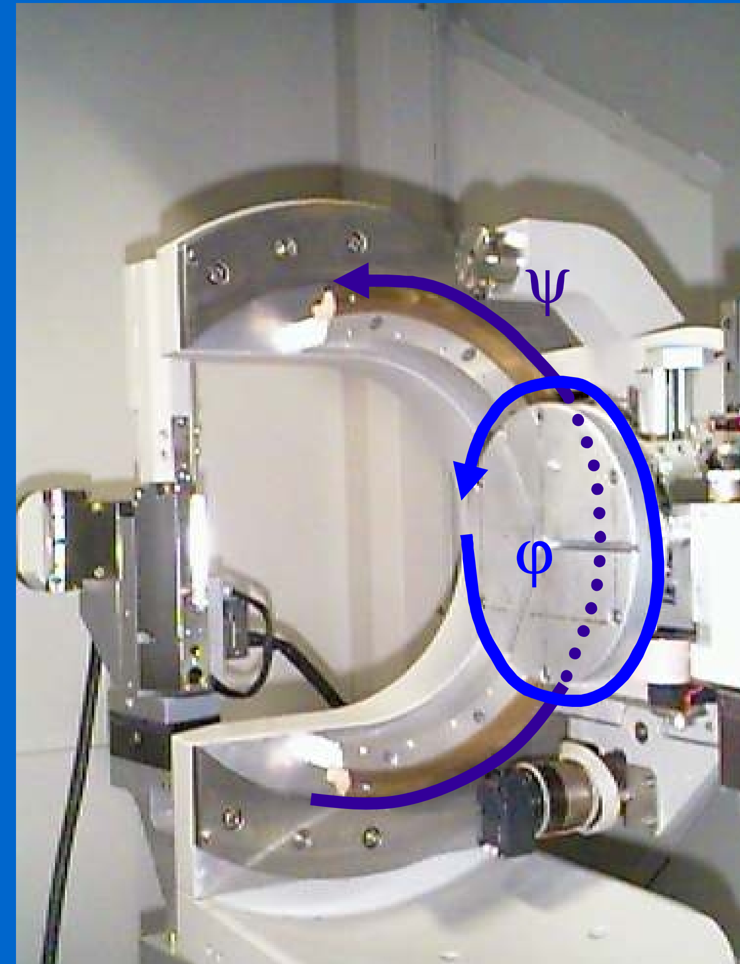

© Do not copy – Do not reproduce

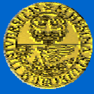

TEXTURE ANALYSIS

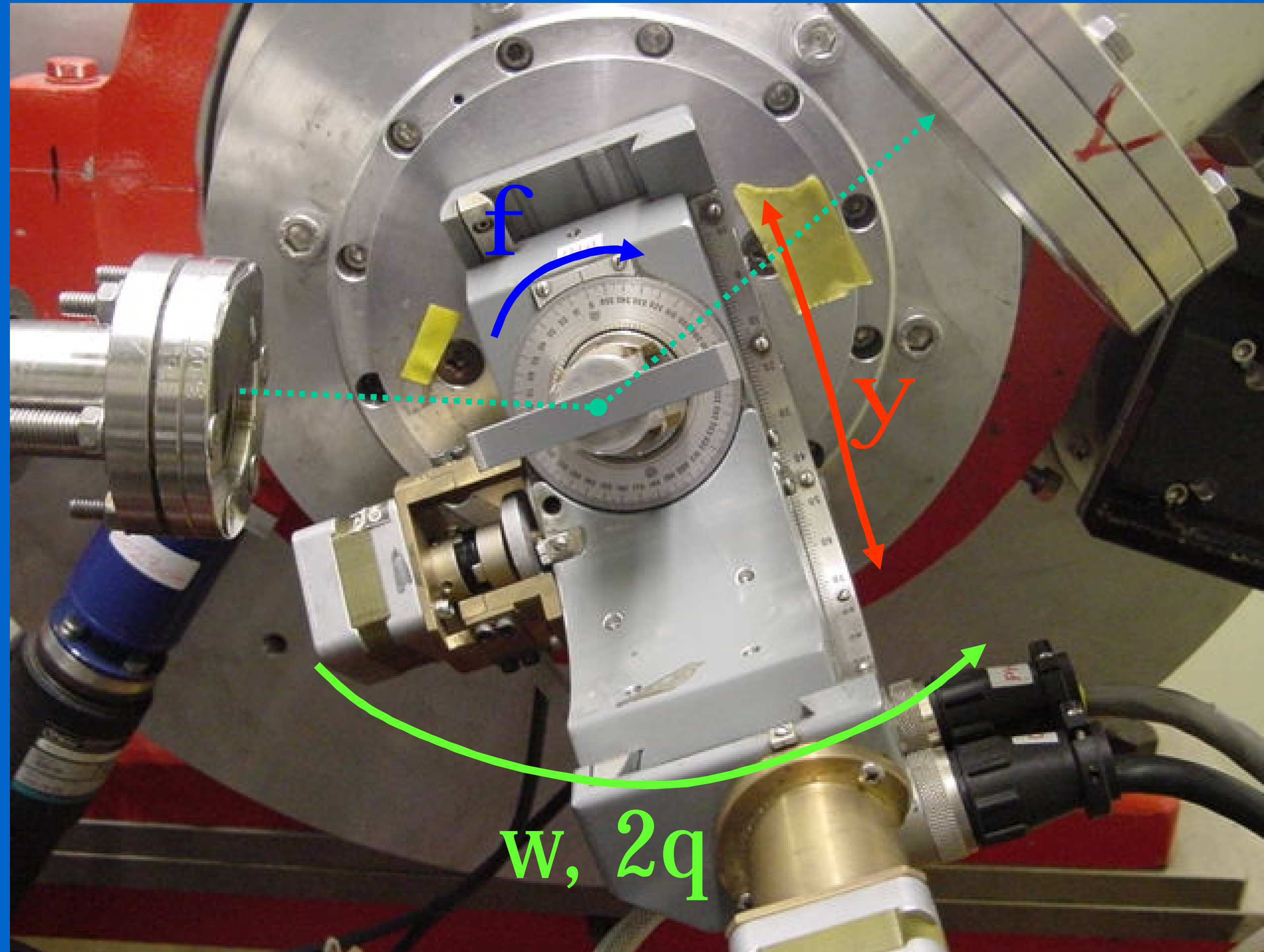

Eulerian cradle for stress/texture measurement: SR XRD instrum.

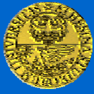

TEXTURE ANALYSIS

Crystallographic texture: pole figures

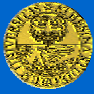

TEXTURE ANALYSIS

In general, texture can be quite complex. Several pole figures, for different (hkl), may be required to understand the orientation

(111) (200) (220)

RD RD RD

Cold-rolled Ni for high-Tc superconducting wires

XRD – A SURVEY OF THE MAIN APPLICATIONS

‘Special techniques’

In situ measurements (high T, p, controlled atmosphere)

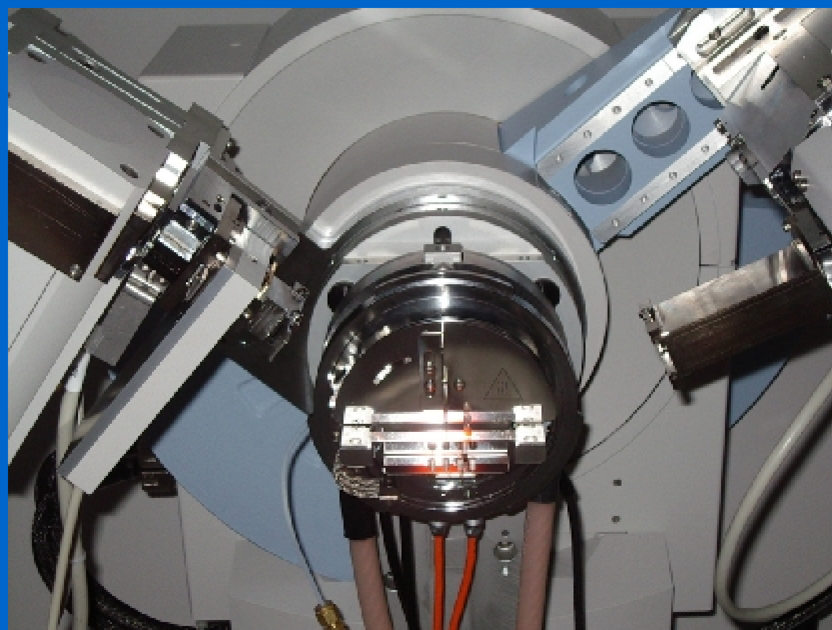

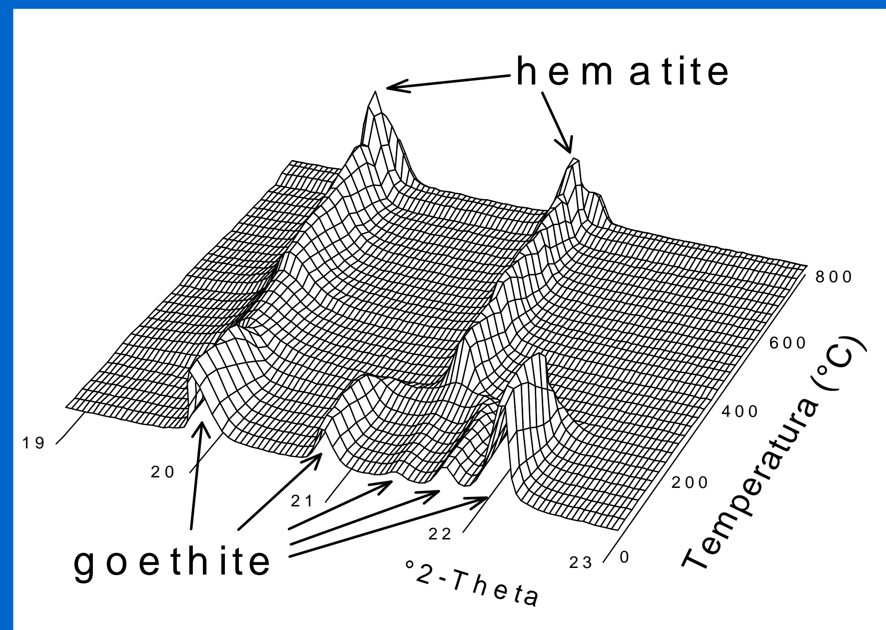

© Do not copy – Do not reproduce

XRD – A SURVEY OF THE MAIN APPLICATIONS

'Special techniques'

Thin film and surface analysis

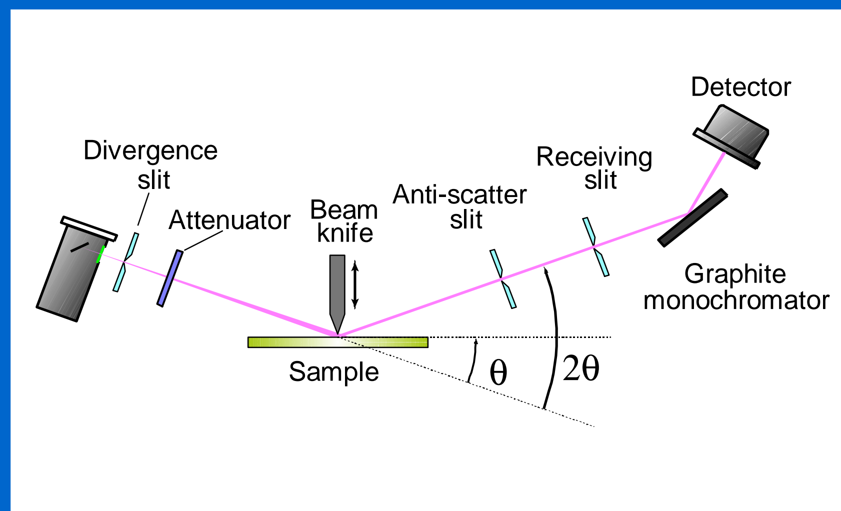

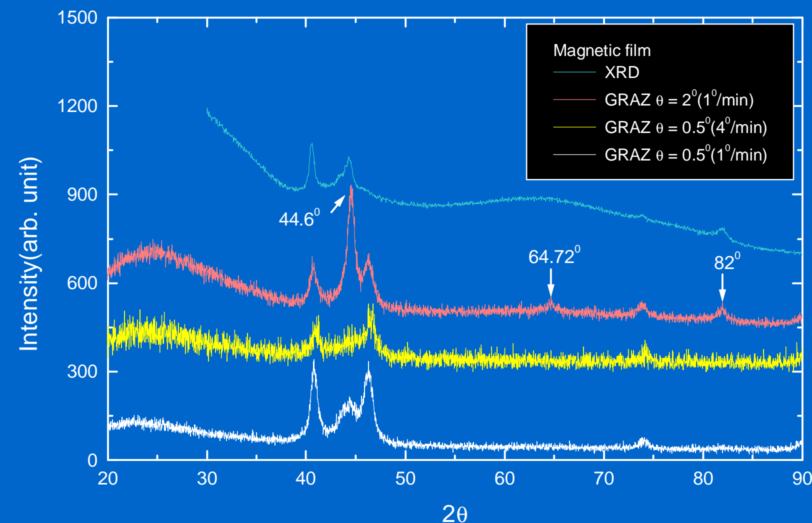

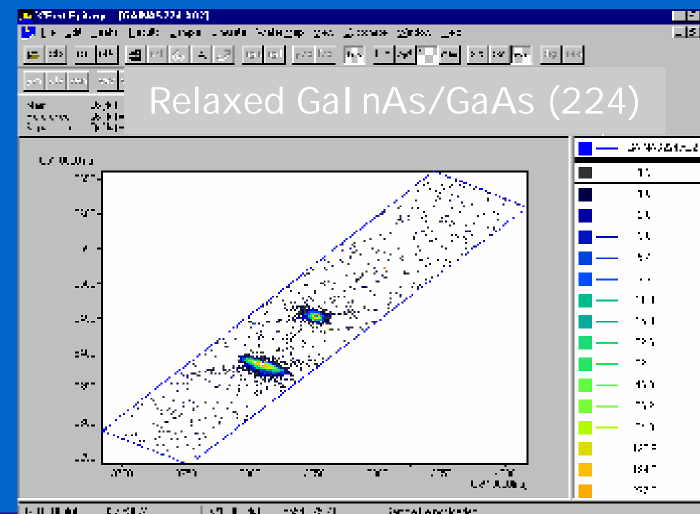

Line Profile Analysis

à PART III

© Do not copy – Do not reproduce